Cell Stem Cell

CellPress

Letter

Murine bone marrow macrophages and human monocytes do not express atypical chemokine receptor 1

Antal Rot,[1,2,3,*] Julia C. Gutjahr,[1] Aindrila Biswas,[3] Maria Aslani,[3] Elin Hub,[1,2] Aude Thiriot,[4,5] Ulrich H. von Andrian,[4,5] Remco T.A. Megens,[3,6] Christian Weber,[3,6,7,8] and Johan Duchene[3,7,*]

[1]Centre for Microvascular Research, William Harvey Research Institute, Barts and The London School of Medicine and Dentistry, Queen Mary University of London, Charterhouse Square, London EC1M 6BQ, UK

[2]Centre for Inflammation and Therapeutic Innovation, Barts and The London School of Medicine and Dentistry, Queen Mary University of London, Charterhouse Square, EC1M 6BQ London, UK

[3]Institute for Cardiovascular Prevention, Ludwig-Maximilians University, Pettenkoferstrasse 8a & 9, 80336 Munich, Germany

[4]Department of Immunology & HMS Center for Immune Imaging, Harvard Medical School, Boston, MA 02115, USA

[5]Ragon Institute of MGH, MIT and Harvard, Cambridge, MA USA

[6]Cardiovascular Research Institute Maastricht, University of Maastricht, P. Debeyelaan, 6229HX Maastricht, the Netherlands

[7]German Center for Cardiovascular Research (DZHK), partner site Munich Heart Alliance, Pettenkoferstrasse 8a & 9, 80336 Munich, Germany

[8]Munich Cluster for Systems Neurology (SyNergy), Pettenkoferstrasse 8a & 9, 80336 Munich, Germany

*Correspondence: a.rot@qmul.ac.uk (A.R.), johan.duchene@med.uni-muenchen.de (J.D.)

https://doi.org/10.1016/j.stem.2021.11.010

The atypical chemokine receptor 1 (ACKR1) was discovered on erythrocytes as the Duffy blood group antigen (Cutbush et al., 1950), also called Duffy-antigen/receptor for chemokines, or DARC (Novitzky-Basso and Rot, 2012). Erythrocytes are terminally differentiated anuclear cells with no transcription and limited translation. Accordingly, within the erythroid lineage ACKR1 expression occurs first and is the highest in erythroblasts (Duchene et al., 2017). Additionally, ACKR1 expression characterizes venular endothelial cells (ECs) (Pruenster et al., 2009; Thiriot et al., 2017), including those lining bone marrow (BM) sinusoids (Duchene et al., 2017). This well-established, distinctive pattern of cell expression has been directly challenged by a publication purporting ACKR1 expression in mouse BM by macrophages, but not erythroblasts and ECs, suggesting that macrophage ACKR1 engages its non-cognate ligand CD82 on hematopoietic stem cells (HSCs) to maintain their quiescence (Hur et al., 2016). In light of the extensive literature, these findings have been particularly provocative, as this was the first description of ACKR1 expression by any leukocyte type and, if correct, would change current concepts of ACKR1 involvement in pathophysiology. The reported ACKR1 expression by macrophages in Hur et al. relied on using commercial anti-ACKR1 antibody FAB6695, which has neither been validated by the manufacturer nor by the authors. This prompted us to investigate the specificity of FAB6695 and scrutinize the apparent ACKR1 expression in BM macrophages.

According to a comprehensive murine BM transcriptome database (https://gexc.riken.jp/), ACKR1 mRNA accumulates in nucleated erythroid cells (NECs), whereas all non-erythroid nucleated cells (NENCs) are devoid of it (Figure S1A). First, we used flow cytometry to probe FAB6695 staining of these two populations. Whereas ACKR1-specific antibody 6B7 (Duchene et al., 2017; Thiriot et al., 2017) accurately discriminated between NECs and NENCs, FAB6695 stained both cell populations almost equally (Figure S1B), as also revealed by their respective staining indices (Figure S1C). Additionally, in contrast to 6B7, FAB6695 immunostained NECs of both wild-type (WT) and ACKR1-deficient (KO) mice (Figure S1D), as reflected by the antibodies' specificity indices (Figure S1E). Next, we compared the staining properties of FAB6695 and 6B7 using an unbiased t-SNE analysis of all BM cells of WT and KO mice. It confirmed that, in contrast to control 6B7, FAB6695 marked NECs and other BM cells equally well and failed to discriminate between WT and ACKR1 KO cells (Figure S1F), corroborating its lack of sensitivity and specificity, respectively. Furthermore, FAB6695 failed to immunodetect ACKR1 on venular ECs in tissue sections (Figure S1G). These data clearly invalidate FAB6695, as it is neither sufficiently sensitive to detect ACKR1 on NECs and ECs nor specific, as it recognizes unrelated epitope(s) present in ACKR1-deficient cells.

Uncovering the unspecific nature of FAB6695 undermined the assertion of ACKR1 expression in BM macrophages and prompted us to address this question directly by staining the whole BM with ACKR1-specific 6B7, co-staining with a broad set of markers and visualizing the results by t-SNE. Unexpectedly, in addition to all NECs, 6B7 marked a subset of F4/80^{pos} macrophages, separating them into two subpopulations (Figure S1H). One, F4/80^{pos}ACKR1^{neg}, co-expressed myeloid markers, CD11b, Ly6C, and CEACAM1, while another, F4/80^{pos}ACKR1^{pos}, did not, though it co-expressed erythroid-specific Ter119 and CD71. Gating on F4/80^{pos} BM cells confirmed that ACKR1^{pos} cells also expressed erythroid-specific markers CD71 and Ter119 (Figure S1I). Moreover, gating on all ACKR1^{pos} cells retrieved only cells with a complete erythroid signature (Figure S1J). Together these data suggested that either a subset of F4/80^{pos} macrophages expressed erythroid-specific surface markers, or, *vice versa,* a subset of NECs expressed F4/80. To clarify the nature of the F4/80^{pos} ACKR1^{pos} cells, we visualized them by imaging flow cytometry, thus revealing that they were not individual cells but cell aggregates comprising at least one ACKR1^{pos}CD71^{pos}Ter119^{pos} NEC and one F4/80^{pos}CD11b^{neg} macrophage

(Figure S1K, Lanes 1–4). NECs and macrophages are spatially and functionally interconnected within the BM erythroblastic islets, each of which comprises a F4/80^{pos}CD11b^{neg} macrophage (Li et al., 2019) surrounded by several adherent NECs (Chasis and Mohandas, 2008). The tight bonds between these cells evidently persist also *ex vivo*, upon their isolation. Conversely, F4/80^{pos}CD11b^{pos} macrophages did not form complexes with NECs and were completely devoid of membrane ACKR1 immunoreactivity (Figure S1K, Lane 5), but few emitted a faint intracellular signal (Figure S1K, Lane 6) that is entirely consistent with an autofluorescence or a spillover from the CD11b channel. The F4/80^{pos}CD11b^{pos} macrophages in the BM, spleen, and peritoneum are known to produce autofluorescent signals. Egregious examples misinterpreting macrophage autofluorescence as immunoreactivity include, e.g., alleging macrophage expression of FoxP3 (Li et al., 2012). Another well-documented artefact associated with immunostaining macrophages results from a non-specific antibody binding via Fc-receptors, necessitating the use of Fc-block and careful analysis versus appropriate controls.

In conjunction, we used a specific antibody 6B7 to establish that BM macrophages themselves do not express ACKR1. However, macrophages form aggregates with ACKR1^{pos} NECs, which, in conventional flow cytometry, despite stringently set doublet-exclusion gates, are detected as singlets, potentially causing artifactual attribution of ACKR1 expression to macrophages, which can also stem from misinterpreting autofluorescence, fluorescence channel spillover, or antibody binding via Fc-receptors. It is plausible that the flow cytometry phenomenon of NEC/macrophage doublets effectively masquerading as single cells is also mirrored in single-cell transcriptomics. However, this was not the case as a comprehensive hematopoietic single-cell transcriptome database (https://tabula-muris.ds.czbiohub.org/) correctly ascribed the ACKR1 mRNA expression to NECs only (Figure S1L).

Our studies provide evidence that BM macrophages do not express ACKR1. However, it remains possible that the described phenotype of HSC dormancy maintained via CD82 (Hur et al., 2016) still depends on ACKR1, albeit expressed by NECs. NECs and macrophages are also spatially and functionally interconnected within the erythroblastic islets of the BM, each comprising a macrophage surrounded by a number of adherent NECs (Chasis and Mohandas, 2008). Because of this functional nexus, it is possible that macrophage depletion by clodronate, which abolished HSC quiescence (Hur et al., 2016), indirectly affected the erythroid lineage and disrupted ACKR1-mediated direct interactions of NECs with HSCs, shown by us to depend on ACKR1 expression by NECs (Duchene et al., 2017). Therefore, it is possible that the ACKR1-dependent *in vitro* effects on HSC proliferation ascribed to BM macrophages (Hur et al., 2016) were actually induced by the ACKR1^{pos} erythroblasts inconspicuously carried into the *in vitro* experimental setups in complex with the isolated macrophages. If CD82 on HSCs indeed engages ACKR1, it would involve NECs, by far the most prevalent BM cell population with all NECs expressing ACKR1.

Paralleling findings in mouse, Hur et al. used an anti-human antibody FAB4139 to ascribe ACKR1 expression to human blood monocytes. We set out to determine the specificity of FAB4139 by comparing its immunoreactivity with erythrocytes of Duffy-positive and Duffy-negative individuals, controlled by a validated anti-ACKR1 antibody 2C3. In contrast to 2C3, which efficiently distinguished Duffy-positive and Duffy-negative erythrocytes, FAB4139 only weakly immunoreacted with Duffy-positive erythrocytes at the highest concentration tested (Figure S1M) and with negligible specificity (Figure S1N). Instead, FAB4139 strongly marked CD45^{+} leukocytes of both Duffy-positive and Duffy-negative individuals, whereas 2C3 labeled leukocytes of Duffy-positive donors only (Figure S1O). Strong immunoreactivity with leukocytes of Duffy-negative donors combined with low sensitivity for erythrocyte ACKR1 suggests that FAB4139 cross-reacts with an epitope unrelated to ACKR1. Because the ACKR1-specific 2C3 also immunoreacted with CD14^{+} monocytes (Figure S1P), we investigated whether this might be due to the formation of cell complexes between erythrocytes and leukocytes. Indeed, imaging flow cytometry confirmed that this was the case, as each CD14^{+}ACKR1^{+} event corresponded to a cell complex of a monocyte and an erythrocyte (Figure S1Q).

Antibodies are indispensable research tools but many, like FAB6695 and FAB4139, are not fit-for-purpose, because they are not specific for their antigens. It is imperative that all antibodies are validated prior to their use. Currently all commercial anti-mouse ACKR1 antibodies, including sc-27817 (Santa Cruz), also used by Hur et al., remain non-validated, completely undermining the credibility of any results obtained using these reagents. Curiously, due to the propensity of myeloid cells to complex with ACKR1^{pos} erythroid cells, staining with specific anti-ACKR1 antibodies might also lead to an erroneous ascription of ACKR1 immunoreactivity to cells devoid of it. Imaging flow cytometry was required to unmask such cell complexes and unequivocally show that myeloid cells themselves neither express ACKR1 nor acquire ACKR1 immunoreactivity through phagocytosis of ACKR1-expressing cells. Other examples of heterologous cell aggregation causing false attribution of cell-specific immunomarkers include complexes between follicular helper T cells and B cells in mouse lymph nodes (Reinhardt et al., 2009) as well as those between T cells and monocytes (Burel et al., 2019) or B cells (Burel et al., 2020) in human blood. It is likely that phenomena of heterologous cell complexes appearing in the singlet gate and masquerading as unusual cell types are even more widespread, necessitating confirmation by imaging whenever new cell types are described solely based on flow cytometry profiles.

In summary, we show that commercial antibodies FAB6695 and FAB4139 are unspecific and unsuitable for detecting mouse and human ACKR1, respectively. We conclude that BM macrophages do not express ACKR1 and therefore cannot maintain the dormancy of HSCs through the ACKR1-CD82 pathway. The human correlate of this molecular pathway is also unsubstantiated, as monocytes do not express ACKR1.

SUPPLEMENTAL INFORMATION

Supplemental information can be found online at https://doi.org/10.1016/j.stem.2021.11.010.

ACKNOWLEDGMENTS

This work was supported by the Wellcome Trust Investigator Award 200817/Z/16/Z to A.R.; Sinergia grant of the Swiss National Science Foundation CRSII3 160719 to A.R.; Deutsche Forschungsgemeinschaft (DFG) grants INST409/150-1 FUGG to R.T.A.M. and C.W., SFB1123-A1/A10 to C.W. and J.D., and SFB1123-Z1 to R.M.; the European Research Council (ERC) AdG°692511 to C.W.; and the German Centre for Cardiovascular Research (DZHK; 81Z0600202) to C.W.

DECLARATION OF INTERESTS

The authors declare no competing interests.

REFERENCES

Burel, J.G., Pomaznoy, M., Lindestam Arlehamn, C.S., Weiskopf, D., da Silva Antunes, R., Jung, Y., Babor, M., Schulten, V., Seumois, G., Greenbaum, J.A., et al. (2019). Circulating T cell-monocyte complexes are markers of immune perturbations. eLife *8*, e46045.

Burel, J.G., Pomaznoy, M., Lindestam Arlehamn, C.S., Seumois, G., Vijayanand, P., Sette, A., and Peters, B. (2020). The Challenge of Distinguishing Cell-Cell Complexes from Singlet Cells in Non-Imaging Flow Cytometry and Single-Cell Sorting. Cytometry A *97*, 1127–1135.

Chasis, J.A., and Mohandas, N. (2008). Erythroblastic islands: niches for erythropoiesis. Blood *112*, 470–478.

Cutbush, M., Mollison, P.L., and Parkin, D.M. (1950). A New Human Blood Group. Nature *165*, 188–189.

Duchene, J., Novitzky-Basso, I., Thiriot, A., Casanova-Acebes, M., Bianchini, M., Etheridge, S.L., Hub, E., Nitz, K., Artinger, K., Eller, K., et al. (2017). Atypical chemokine receptor 1 on nucleated erythroid cells regulates hematopoiesis. Nat. Immunol. *18*, 753–761.

Hur, J., Choi, J.I., Lee, H., Nham, P., Kim, T.W., Chae, C.W., Yun, J.Y., Kang, J.A., Kang, J., Lee, S.E., et al. (2016). CD82/KAI1 Maintains the Dormancy of Long-Term Hematopoietic Stem Cells through Interaction with DARC-Expressing Macrophages. Cell Stem Cell *18*, 508–521.

Li, W., Wang, Y., Zhao, H., Zhang, H., Xu, Y., Wang, S., Guo, X., Huang, Y., Zhang, S., Han, Y., et al. (2019). Identification and transcriptome analysis of erythroblastic island macrophages. Blood *134*, 480–491.

Li, F., Yang, M., Wang, L., Williamson, I., Tian, F., Qin, M., Shah, P.K., and Sharifi, B.G. (2012). Autofluorescence contributes to false-positive intracellular Foxp3 staining in macrophages: A lesson learned from flow cytometry. J Immunol. Methods *386*, 101–107.

Novitzky-Basso, I., and Rot, A. (2012). Duffy antigen receptor for chemokines and its involvement in patterning and control of inflammatory chemokines. Front. Immunol. *3*, 266.

Pruenster, M., Mudde, L., Bombosi, P., Dimitrova, S., Zsak, M., Middleton, J., Richmond, A., Graham, G.J., Segerer, S., Nibbs, R.J., and Rot, A. (2009). The Duffy antigen receptor for chemokines transports chemokines and supports their promigratory activity. Nat. Immunol. *10*, 101–108.

Reinhardt, R.L., Liang, H.E., and Locksley, R.M. (2009). Cytokine-secreting follicular T cells shape the antibody repertoire. Nat. Immunol. *10*, 385–393.

Thiriot, A., Perdomo, C., Cheng, G., Novitzky-Basso, I., McArdle, S., Kishimoto, J.K., Barreiro, O., Mazo, I., Triboulet, R., Ley, K., et al. (2017). Differential DARC/ACKR1 expression distinguishes venular from non-venular endothelial cells in murine tissues. BMC Biol. *15*, 45.

Cell Stem Cell, Volume *29*

Supplemental Information

Murine bone marrow macrophages and human monocytes do not express atypical chemokine receptor 1

Antal Rot, Julia C. Gutjahr, Aindrila Biswas, Maria Aslani, Elin Hub, Aude Thiriot, Ulrich H. von Andrian, Remco T.A. Megens, Christian Weber, and Johan Duchene

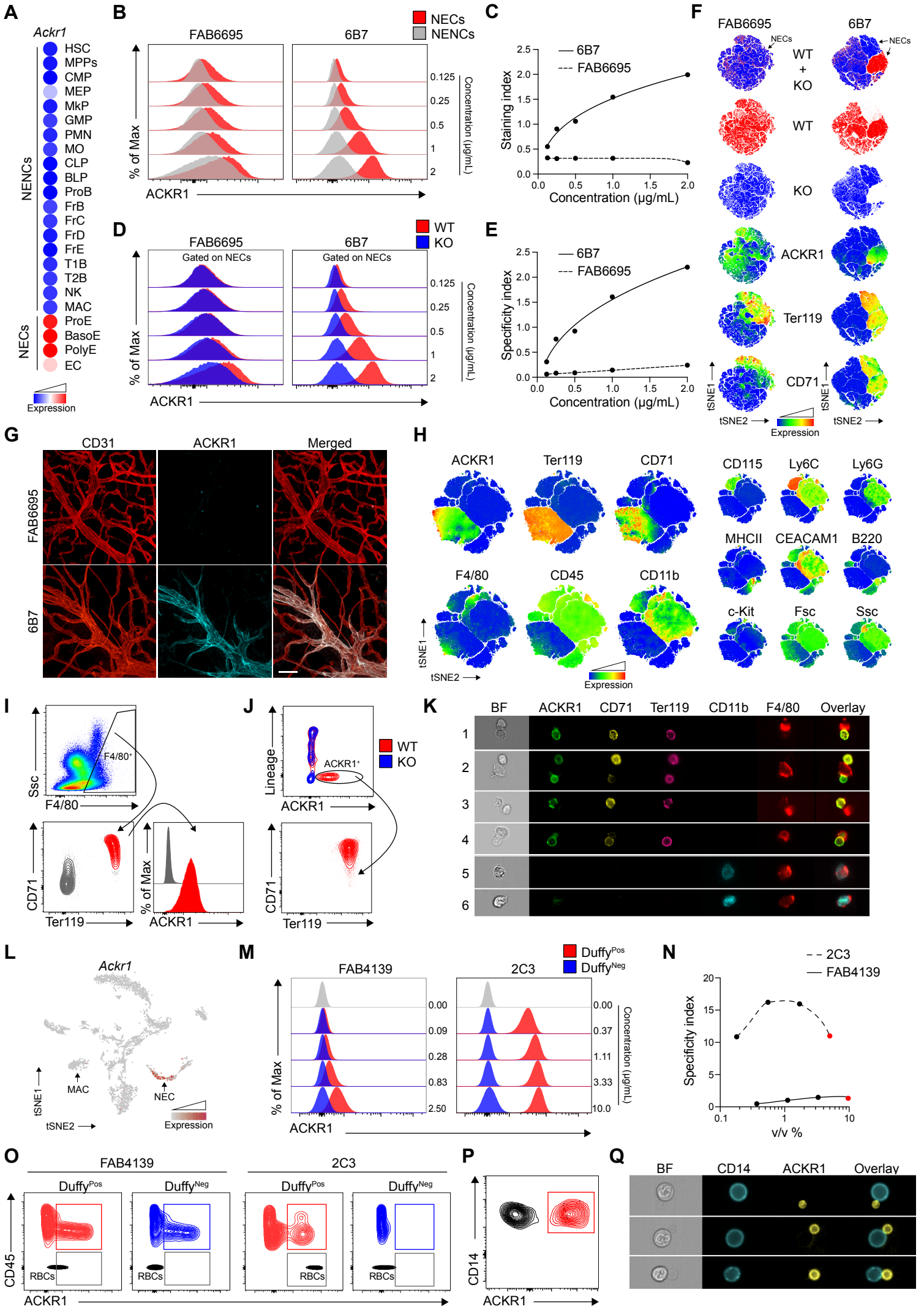
A
Ackr1
HSC
MPPs
CMP
MEP
MkP
GMP
PMN
MO
CLP
BLP
ProB
FrB
FrC
FrD
FrE
T1B
T2B
NK
MAC
ProE
BasoE
PolyE
EC
NENCs
NECs
Expression
B
NECs
NENCs
FAB6695
6B7
% of Max
ACKR1
0.125
0.25
0.5
1
2
Concentration (μg/mL)
C
6B7
FAB6695
Staining index
Concentration (μg/mL)
D
WT
KO
Gated on NECs
E
Specificity index
F
NECs
WT + KO
WT
KO
ACKR1
Ter119
CD71
tSNE1
tSNE2
Expression
G
CD31
ACKR1
Merged
FAB6695
6B7
H
ACKR1
Ter119
CD71
CD115
Ly6C
Ly6G
MHCII
CEACAM1
B220
F4/80
CD45
CD11b
c-Kit
Fsc
Ssc
tSNE1
tSNE2
Expression
I
F4/80⁺
Ssc
F4/80
CD71
Ter119
% of Max
ACKR1
J
WT
KO
ACKR1⁺
Lineage
ACKR1
CD71
Ter119
K
BF
ACKR1
CD71
Ter119
CD11b
F4/80
Overlay
1
2
3
4
5
6
L
Ackr1
MAC
NEC
tSNE1
tSNE2
Expression
M
Duffy^Pos
Duffy^Neg
FAB4139
2C3
% of Max
ACKR1
0.00
0.09
0.28
0.83
2.50
0.37
1.11
3.33
10.0
Concentration (μg/mL)
N
2C3
FAB4139
Specificity index
v/v %
O
FAB4139
2C3
Duffy^Pos
Duffy^Neg
CD45
RBCs
ACKR1
P
CD14
ACKR1
Q
BF
CD14
ACKR1
Overlay

Supplemental Figure 1. Mouse bone marrow macrophages and human blood monocytes do not express ACKR1.

(**A**) Microarray analysis heatmap of *Ackr1* mRNA expression in mouse BM cells: proerythroblasts (ProE), early normoblasts (BasoE), late normoblasts (PolyE), endothelial cells (EC). NECs, nucleated erythroid cells; NENCs, non-erythroid nucleated cells. Source: gexc.riken.jp/models/1649. (**B**) Representative flow cytometry analysis of BM cells of WT mice stained with different concentrations (0.125 – 2µg/mL) of FAB6695 and 6B7. Here and elsewhere NECs were gated as $CD71^{pos}Ter119^{pos}$ and NENCs as $CD71^{neg}Ter119^{neg}$. (**C**) Staining Index curves of FAB6695 and 6B7. Geometric MFI of signals in NECs and NENCs were obtained and used to calculate the Staining Index= $(MFI_{NEC}–MFI_{NENC})/(2xSD_{NENC})$. (**D**) Representative flow cytometry staining of BM NECs from WT and ACKR1-deficient (KO) mice by FAB6695 and 6B7 at 0.125 to 2µg/mL. (**E**) Specificity index curves of FAB6695 and 6B7. Geo MFI values obtained for FAB6695 and 6B7 in WT and KO NECs were used to calculate the Specificity Index=$(MFI_{WT}–MFI_{KO})/(2xSD_{KO})$. (**F**) BM cells of WT (red) and KO (blue) mice combined in t-SNE plots. Expression levels of indicated markers are reflected by a color scale from blue (low expression) to red (high expression). ACKR1 stained by FAB6695 or 6B7. Arrows indicate NECs. (**G**) Representative immunofluorescence micrographs of omentum of WT and KO mice, as assessed by confocal microscopy after staining for CD31 (red) and for AKCR1 with either FAB6695 or 6B7 (blue). Scale bar: 100 µm. (**H**) BM cells of WT mice in t-SNE dimensional reduction based on the expression of 13 immunomarkers. Expression levels are color mapped from blue (low expression) to red (high expression). ACKR1 stained by 6B7. (**I**) *Top*: Representative flow cytometry plot showing the gating strategy based on the F4/80 staining of the whole BM. *Bottom left*: Fraction of NECs (red) from the parental gate. *Bottom right*: Expression of ACKR1 (stained by 6B7) in NECs (red) and remaining NENCs (grey). (**J**) *Top*: Representative flow cytometry plot showing the gating strategy of the whole WT (red) and KO (blue) BM based on ACKR1 expression stained with 6B7. Lineage cocktail contained B220, CD3, CD11b and Gr1 antibodies. *Bottom*: Fraction of NECs from the parental gate. (**K**) Gallery of representative images of $F4/80^{pos}ACKR1^{pos}$ events visualized by imaging flow cytometry; ACKR1 stained by 6B7. BF, Brightfield. (**L**) tSNE graph of mRNA expression of *Ackr1* determined by single cell RNA sequencing of mouse BM cells. NECs and macrophages (MAC) are indicated by arrows. Source: tabula-muris.ds.czbiohub.org. (**M**) Representative flow cytometry analysis of FAB41139 and 2C3 binding at different concentrations to red blood cells (RBCs) from healthy Duffy-positive and Duffy-negative individuals. (**N**) Specificity index curves of FAB41139 and 2C3. Geo MFI values obtained for FAB41139 and 2C3 in Duffy-positive and Duffy-negative RBCs were used to calculate the Specificity Index=$(MFI_{Duffy\text{-}pos}–MFI_{Duffy\text{-}neg})/(2xSD_{Duffy\text{-}neg})$. Red dots represent antibody concentrations recommended as optimal by the providers. (**O**) Representative flow cytometry analysis for binding of FAB41139 and 2C3 to white blood cells (WBCs) from Duffy-positive and Duffy-negative individuals. WBCs were gated as $CD45^{pos}$ cells. (**P**) Representative flow cytometry plot of $CD14^{pos}ACKR1^{pos}$ events from Duffy-positive donor blood reacted with 2C3. (**Q**) Gallery of representative images of $CD14^{pos}ACKR1^{pos}$ events visualized by imaging flow cytometry, ACKR1 stained by 2C3. BF, brightfield.